scientific reports

Check for updates

OPEN

A novel biomarker of COVID-19: MMP8 emerged by integrated bulk RNAseq and single-cell sequencing

Zhenguo Liu[1] & Shunda Wang[2]✉

COVID-19 has been emerging as the most influential illness which has caused great costs to the heath of population and social economy. Sivelestat sodium (SS) is indicated as an effective cure for lung dysfunction, a characteristic symptom of COVID-19 infection, but its pharmacological target is still unclear. Therefore, a deep understanding of the pathological progression and molecular alteration is an urgent issue for settling the diagnosis and therapy problems of COVID-19. In this study, the bulk ribonucleic acid sequencing (RNA-seq) data of healthy donors and non-severe and severe COVID-19 patients were collected. Then, target differentially expressed genes (DEGs) were screened through integrating sequencing data and the pharmacological database. Besides, with the help of functional and molecular interaction analyses, the potential effect of target gene alteration on COVID-19 progression was investigated. Single-cell sequencing was performed to evaluate the cell distribution of target genes, and the possible interaction of gene-positive cells with other cells was explored by intercellular ligand-receptor pattern analysis. The results showed that matrix metalloproteinase 8 (MMP8) was upregulated in severe COVID-19 patients, which was also identified as a targeting site to SS. Additionally, MMP8 took a core part in the regulatory interaction network of the screened DEGs in COVID-19 and was dramatically correlated with the inflammatory signaling pathway. The further investigations indicated that MMP8 was mainly expressed in myelocytes with a high degree of heterogeneity. MMP8-positive myelocytes interacted with other cell types through RETN-TLR4 and RETN-CAP1 ligand-receptor patterns. These findings emphasize the important role of MMP8 in COVID-19 progression and provide a potential therapeutic target for COVID-19 patients.

Keywords COVID-19, Single-cell sequencing, MMP8, RNA sequencing, Cell-to-cell communication

Severe acute respiratory syndrome coronavirus-2 (SARS-CoV-2)-induced disease, also called COVID-19, has being a widely spread epidemic infection in the world in these years[1]. The high infection rate and severe rate of such a disease have burdened general household health and social economy a lot[2]. In response to the epidemic of COVID-19, a series of prevention and control measures have been taken, including keeping social distance, wearing a mask, frequently washing hands, etc[3]. Sivelestat sodium (SS), a specific inhibitor drug of neutrophil elastase, is indicated as an effective cure for various inflammatory disorders, such as lung injury, myocarditis, and knee osteoarthritis[4–6]. Interestingly, SS was preliminarily applied in clinical treatment of COVID-19 patients due to its improved effects on pneumonia, acute respiratory distress syndrome and severe lung dysfunction, characteristic symptoms of SARS-Cov-2 infection[7,8]. Nevertheless, the specific mechanism of SS in mediating COVID-19 pathogenesis is unclear. Deeply investigating the alteration of body reactivity and potential infectious mechanism, as well as latent SS targeting markers, is still an urgent issue for the prevention and therapy of COVID-19.

The diagnosis strategy of COVID-19 is mainly based on SARS-CoV-2 detection using blood, swabs from nasopharynx, and saliva samples from patients[9]. The target genome complementary to virus, specific antibody interacted with virus antigen and neutralized antibody associated with recombinant antigen are the underlying basis for COVID-19 diagnosis[10]. The lungs are typically the primary organs impacted by SARS-CoV-2, largely due to their extensive and highly vascularized surface area[11]. Various biomarkers linked to different phases of lung involvement in COVID-19 have been discovered, showing a correlation with both pulmonary and systemic hyperinflammation as well as fibrotic injury[12]. During the initial phases of the illness, neuron-specific enolase can assist in identifying patients who are likely to experience dyspnea[13]. At the time of admission,

[1]Department of Intensive Care Unit, Shaanxi Provincial People's Hospital, Xi'an 710068, Shaanxi, China. [2]Department of Rehabilitative medicine, Shaanxi Provincial People's Hospital, No.256, Youyi West Road, Beilin District, Xi'an 710068, Shaanxi, China. ✉email: wanda0916@126.com

elevated lymphocyte and platelet levels, combined with decreased concentrations of ferritin, D-dimer, lactate dehydrogenase, and aspartate transaminase, have been associated with a lower risk of death in COVID-19 patients who eventually required intubation and mechanical ventilation[14]. Levels of surfactant protein-D, angiopoietin-2, and triggering receptors expressed on myeloid cells (TREM)-1 and TREM-2 were found to be higher in patients with mild/moderate and severe/critical COVID-19 pneumonia compared to those who were asymptomatic or had uncomplicated cases[15]. Moreover, the alterations in immunity responses, such as immune cell exhaustion and dysregulated inflammatory cytokine production presenting in the peripheral blood, are dominant causes that trigger the imbalance of protection measures in the body intruded by SARS-CoV-2[16,17]. It is crucial to better understand the pathophysiological development of COVID-19 for discovering more effective treatments. Current research has validated several potential regulators for immune activity in human under COVID-19 infection[18,19]. However, there still lacks the evidence on available COVID-19 biomarkers and pharmacological target in clinic.

It is well-known that the valuable advantages of metagenomic next-generation sequencing are quickly delineating the microbiome of patients, looking for the co-targets of sample detection sites, and furtherly guiding to obtain an approach impacting patients' outcome[20,21]. Hereinto, the high throughout bulk transcriptome sequencing is characterized by simultaneous analysis of large-scale gene data[22]. There also exists limitations in traditional bulk ribonucleic acid sequencing (Bulk-seq) yet. For instance, the expression profile of target genes is at the average level in cell population without considering the heterogeneity of different cell types[23]. In recent years, integrated Bulk-seq and single-cell RNA sequencing (scRNA-seq) analysis is becoming a prevailing manner to understand the progression and mechanism of immune responses as a result of the emerging development of scRNA-seq settling such problems to some extent[24]. However, less findings have been discovered nowadays in targeting to the genomic alteration of COVID-19 patients.

In the present research, an integrated analysis was conducted on differentially expressed genes (DEGs) originated from COVID-19 patients at various stages and candidate genes of SS collected from a pharmacological database to screen target genes. Except for evaluating the structure, function and interaction of target genes, their single-cell expression profile and specific cell distribution, as well as the dynamic state of heterogeneous cells, in COVID-19-infected samples were also analyzed. This study may propose specific targets for COVID-19 and facilitate immune diagnosis and therapy developments for such patients.

Materials and methods

Ethics approval and informed consent form

This study was approved by the Ethics Committee of Shaanxi Provincial People's Hospital (no. SPPH-LLBG-17-3_2). This was a retrospective study, for which formal consent is not required. All methods were performed in accordance with the relevant guidelines and regulations.

Bulk-seq data collection and analysis

The bulk-seq expression profile and relevant clinical data of healthy donators and COVID-19 patients at various stages were collected from the gene expression omnibus (GEO, https://www.ncbi.nlm.nih.gov/geo/) with an accession number of GSE213313[25].

Analysis of DEGs by bulk-seq

Then, the bulk-seq expression profile was preprocessed by background correction, gene symbol transformation and normalization using RStudio (ver. 4.2.0, https://www.r-project.org/) programming. The limma package[26] was utilized for screening the significant DEGs in these datasets. Significant DEGs referred to those with the absolute of log2 fold change ($\log_2$FC) > 1 and the adjust P value < 0.05.

Pharmacological target screening and molecular docking analysis

The 2D and 3D molecule structures of SS with compound CID number of 107,706 were available from the PubChem database (https://pubchem.ncbi.nlm.nih.gov/). Then, the 2D structure of SS was loaded to the PharmMapper database (https://www.lilab-ecust.cn/pharmmapper/), which was used to analyze the possible binding sites of SS. Eventually, the intersection between binding sites and significant DEGs was utilized to identify pharmacological targets.

The 2D and 3D molecule structures of the candidate pharmacological target matrix metalloproteinase 8 (MMP8) with PDB number of 1A85 were available from the RCSB protein bank (https://www.pdb.org/). To analyze the binding affinities and modes of interaction between the SS and MMP8, Autodock Vina 1.2.2 (http://autodock.scripps.edu/), a silico protein–ligand docking software, was employed. For docking analysis, all protein and molecular files were converted into PDBQT format with all water molecules excluded and polar hydrogen atoms added. The grid box was centered to cover the domain of each protein and to accommodate free molecular movement. The grid box was set to 30 Å × 30 Å × 30 Å, with a grid point distance of 0.05 nm. Molecular docking studies were performed by Autodock Vina 1.2.2.

Weighted correlation network analysis (WGCNA)

To illuminate the correlation network of MMP8 in COVID-19, the WGANA was employed. Firstly, the 1,210 significant DEGs derived from differential analysis between severe COVID-19 group and healthy group were evaluated and tested for availability. Using WGCNA R package[27] and adjacency matrix formula [sij = |cor (xi, xj)|aij = $Sij\beta$, where i and j stood for DEGs, xi and xj were expression levels, and sij and aij were correlation coefficient and strength, respectively), a co-expression network and an adjacency matrix describing correlation strength were constructed. Then, a topological overlap matrix was formed based on above-mentioned analysis data. To identify the specific module, hierarchical clustering was conducted and correlation between modules

and MMP8 expression was calculated. Eventually, the specific module possessing the highest correlation with MMP8 was regarded as the co-expression module.

To evaluate the critical position of MMP8 in the co-expression module, the protein-protein interaction (PPI) analysis was performed based on the String database (https://string-db.org/), and the Cytoscape tools (https://cytoscape.org/) were used to estimate the hub genes with molecular complex detection (MCODE) algorithm.

Functional annotation analyses

The candidate genes resulting from differential analysis between severe COVID-19 group and healthy group or the co-expression module were used for gene ontology (GO) analysis, Kyoto encyclopedia of genes and genomes (KEGG) analysis, and gene set enrichment analysis (GSEA) using the clusterprofiler package[28], and the results met the requirements with adjust P value < 0.05.

ScRNA-seq data collection and analysis

The Chromium 10X scRNA-seq expression profile and relevant clinical data of 33 periphery blood samples derived from healthy donors and COVID-19 patients at different stages were collected from the GEO with an accession number of GSE157344[29].

The gene expression matrix and corresponding clinical data of the 33 periphery blood samples were imported in the RStudio (ver.4.2.0) and further analyzed by the Seurat package[30]. Downstream analysis was performed with primary expression data, and low-quality single cells containing < 300 expressed genes or > 10% mitochondrial transcripts or > 0.5% red cell transcripts were filtered out. Besides, genes expressed in fewer than 3 single cells were also eliminated. Following the exclusion of low-quality cells, the expression data of remaining 56,814 single cells were normalized, and top 5000 highly variable features were selected with variance stabilizing transformation method. Next, the gene expression was further subjected to z-score transformation using linear method to scale and center the top 5000 highly variable features in this dataset. Afterwards, the principal component analysis (PCA) was performed to reduce the dimensionality of the data using the top 5,000 most variable genes in the dataset. After that, the first 20 PCs were used for downstream calculation based on FindNeighbors using default parameters. The resolution parameter of 0.5 determined between 0.1 and 1 depending on the single cell dataset was used to identify clusters. The t-distributed stochastic neighbor embedding (t-SNE) was applied for non-linear dimensionality reduction to determine and visualize various single cell clusters. The marker genes for individual clusters were calculated, and only top 3 significantly upregulated genes (adjust P value < 0.05, minimal percentage > 0.25, and $\log_2$FC > 0.25) were presented by heatmap. Subsequently, the SingleR algorithm and Cellmarker dataset (http://bio-bigdata.hrbmu.edu.cn/CellMarker/index.html) were jointly employed to annotate the cell type of various single cell clusters[31,32].

Cell-to-cell communication analysis of scRNA-seq data

Cell-cell interaction is critical for diverse cellular destiny via soluble and membrane-bound factors, such as regulation of cell cycle, migration or differentiation[33]. To investigate the communicating interactions between different cell types and identify the mechanism of communicating molecules in this scRNA-seq, CellChat package was applied using default parameters[34].

Participants and samples preparation

A total of 10 critical COVID-19 patients admitted to intensive care unit, 10 non-critical COVID-19 patients and 10 healthy donors were enrolled in this study. The clinical characteristics of the severe or mild patients was defined according to these standards: assigned score 1 and 2 for non-hospitalized patients with no activity limitations, respectively; assigned score 3 and 4 for hospitalized patients who did not utilize oxygen therapy via mask, respectively; assigned score 5 and 6 for hospitalized patients who required non-invasive ventilation/intubation and mechanical ventilation, respectively; assigned score 7 for hospitalized patients requiring multi-organ support. The non-critical stage was scored 3 or 4, while the critical patients was scored 6 or 7.

Peripheral blood derived from COVID-19 patients and healthy donors were gathered in EDTA-coated tubes, respectively. In brief, 3 ml of peripheral blood was washed twice with PBS and the red cell lysis was used twice with 15 mL of 0.2% NaCl solution, while was blocked by using 35 mL of 1.2% NaCl solution. The remain cells were washed with PBS, resuspended in RPMI 1640 medium supplemented with 5% bovine serum albumin.

Total RNA was extracted from cells with Trizol reagent (Invitrogen, CA, USA) and the concentration was determined. The cDNA was synthesized using a reverse transcription kit (Genechem, Shanghai) according to the instructions and then qRT-PCR was performed, with GAPDH as the internal reference. The $2^{-\Delta\Delta Ct}$ method was used to calculate the expression of relevant genes. The primer sequences are as follows: MMP8 (forward): 5′-GGAAGGCAGGAGAGGTTGTC–3′, MMP8 (reverse): 5′--GTTGAAAGGCATGGGCAAGG-3′; GAPDH (forward): 5′-CACCATTGGCAATGAGCGGTTC-3′, GAPDH (reverse): 5′-AGGTCTTTGCGGATGTCCAC GT-3′.

The RIPA buffer (Qiagen, NRW, Germany) lysed tissues to obtain the total protein, and the BCA protein assay kit (Thermo Fisher Scientific, MA, USA) was used to analyze the protein concentration. Each protein samples were subjected to 10% SDS-PAGE, transferred to PVDF membranes (Millipore, MA, USA) and incubated overnight at 4 °C with primary antibodies against MMP8 and GAPDH (ab81286, ab9482, Abcam, USA). Following this, the PVDF membrane was washed three times with TBST (Thermo Fisher Scientific, MA, USA) and incubated with HRP-conjugated secondary antibody (#7074, CST, USA) for 1 h at room temperature. The signal was shown by the enhanced chemiluminescence immunoblotting detection reagent (Thermo Fisher Scientific, MA, USA).

Statistical analysis

RStudio was employed for statistical analysis. The significance test methods of different analyses were determined by corresponding packages. The two-sided $P < 0.05$ was considered statistically significant.

Results

DEGs between COVID-19 patients and healthy subjects identified by bulk RNA-seq

To explore the significant DEGs during COVID-19 progression, 94 subjects including 11 healthy donors and 50 severe and 33 non-severe COVID-19 patients were enrolled, and their sequencing data were analyzed. The results presented that there existed 735 up-regulated and 475 down-regulated significant DEGs between severe group and healthy group, while 39 significant DEGs were up-regulated and 12 were down-regulated between non-severe group and severe group (Fig. 1A and B). Thirty-five significant DEGs were identified in the non-severe COVID-19 group with non-severe group and healthy group simultaneously (27 up-regulated and 8 down-regulated ones, Fig. 1C). SS is an effective anti-lung injury drug in clinical practice, which has been used for alleviating the acute respiratory distress syndrome of COVID-19 patients and achieves significant clinical benefits[8,35]. In that case, the PharmMapper database, a pharmacophore matching and potential identification target platform, was jointly utilized to further screen targets of SS for COVID-19, and a total of 248 candidate pharmacological sites with normalization fit score > 0.5 were identified as credible targets (Fig. 1D and E). Ultimately, only MMP8 was considered as a potential target upregulated in severe COVID-19 patients (Fig. 1F). Subsequently, the up-regulation of MMP8 was verified to be associated with the severe progression of severe COVID-19 in a symptom duration-dependent manner (Fig. 1G, $P < 0.05$, $P < 0.01$, $P < 0.001$). However, the tendency was not significant in non-severe COVID-19 patients (Fig. 1H, $P > 0.05$, $P < 0.01$, $P < 0.001$). To validity the mRNA expression and protein level in our samples, the qRT-PCR and western blotting were used to examine. The results showed that the mRNA expression and protein level of MMP8 were both elevated in critical COVID-19 patients (Fig. 1I and J, $P < 0.01$, $P < 0.001$). These evidences suggested the potential value of MMP8 to indicate the severity of COVID-19 and serve as a therapy target of SS.

Analysis of targeted binding between MMP8 and SS

To evaluate the affinity of SS for MMP8, molecular docking analysis was conducted. The binding poses and interactions of SS with MMP8 protein were obtained with Autodock Vina v.1.2.2, and binding energy was generated. The results revealed that SS bound to MMP8 through visible hydrogen bonds and strong electrostatic interactions in top 3 lower binding energy, which indicated highly stable binding (− 7.828, − 7.811 and − 7.658 kcal/mol). Moreover, the hydrophobic pocket of MMP8 protein was occupied successfully by SS (Fig. 2A–C).

Analysis on co-expression network of MMP8 in COVID-19

Next, WGCNA was conducted using Cytoscape to identify the co-expression network of MMP8 in COVID-19 based on the above mentioned DEG matrix. A scale free network was built with a soft threshold calculated to 9 with the R^2 value at 0.9 (Fig. 3A and B). The network heatmap showed the clustered DEGs, and great positive correlation was found between MMP8 expression and the eigengenes in black module according to WGCNA (Fig. 3C–E). Moreover, the 55 intra-module genes also presented a satisfactory correlation coefficient (Fig. 3F, $r = 0.90$, $P < 0.001$), which indicated that these genes compose a complicated and reliable co-expression network to affect COVID-19 progression. Then, the String database was used to construct a PPI network between MMP8 and the eigengenes in black module. According to Fig. 3G, there existed 54 DEGs interacting with MMP8, with darker lines possessing more credible interaction. Notably, the 21 genes were identified as the core network by MCODE method in Cytoscape platform, with the MMP8, CSTG, BPI, ELANE and MPO located in the critical position of the core network according to maximal clique centrality method (Fig. 3H). The CSTG, BPI, ELANE and MPO were indicated as crucial factors participating in immune disorders and infections, which ulteriorly suggested that MMP8 may be a central gene in mediating COVID-19 progression, in line with the findings in previous studies[36–38],.

Analyses on regulatory mechanism and corresponding pathway of MMP8 during COVID-19 progression

Integrated enrichment analyses were subsequently conducted to investigate the regulatory mechanism of MMP8 based on these 54 core DEGs in COVID-19. The results of GO enrichment analysis indicated that MMP8 was most significantly associated with several increased cellular processes, with the formation of vesicle lumen, cytoplasmic vesicle lumen, secretory granule lumen, specific granule and specific granule lumen as the top 5 ones (Fig. 4A). The results of KEGG analysis presented that MMP8 was dramatically related to neutrophil extracellular trap (NET) formation (Fig. 4B). Besides, GESA enrichment analysis results revealed that MMP8 had great correlations with most of the activated inflammatory pathways, such as the interferon response, G2M checkpoint, STAT3 and NF-κB pathways (Fig. 4C and D).

MMP8-positive cell subpopulations in COVID-19

ScRNA-seq was further utilized to investigate MMP8-positive cells in COVID-19 pathogenesis. The results showed that there was 1 kind of cell subpopulation in COVID-19 specimens (Fig. 5A). According to the cross-referenced specific factors and identified bio-markers in cell clusters, the cell subpopulation was validated to have a total of 10 known types, including immature B cells, naive B cells, cluster of differentiation 16 $(CD16)^-$ monocytes, $CD16^+$ monocytes, myelocytes, neutrophils, natural killer (NK) cells, platelets, $CD4^+$ central memory T cells and γ-δ T cells (Fig. 5B and C). Next, the distribution of cells specifically expressing MMP8 was assessed, and it was found that MMP8 was highly expressed in the myelocyte cluster. Moreover, the proportion of myelocytes rose sharply, while that of $CD4^+$ central memory T cells declined in severe COVID-19 group

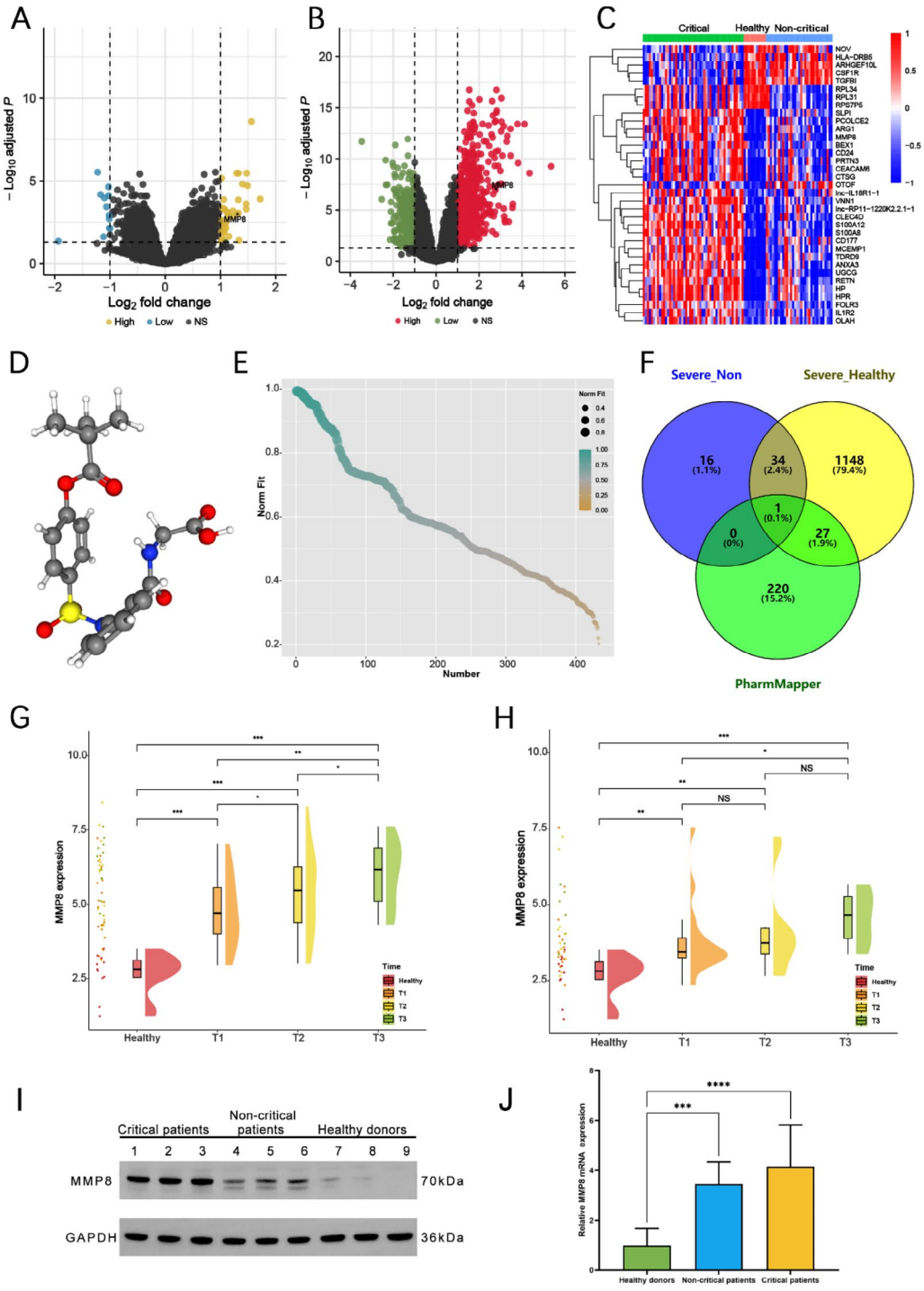

Fig. 1. Analysis of DEGs during COVID-19 progression. (**A**, **B**) Volcano diagram showing the profile of DEGs between healthy group and severe COVID-19 group (**A**), as well as healthy group and non-severe COVID-19 group (**B**), and the expression profile was extracted from the GSE213313 database. DEGs were defined as $\log_2$FC > 1 and the adjust *P* value < 0.05. (**C**) The hierarchical bi-clustering analysis indicated significant DEGs. (**D**) 3D structure of SS from PubChem. (**E**) The normalization fit score of pharmacological sites from Pharmmapper. (**F**) Venn diagram showing the DEG components from different datasets. (**G**) Expression of MMP8 in the blood samples of severe COVID-19 patients at different pathological phases. (**H**) Expression of MMP8 in the blood samples of non-severe COVID-19 patients at different pathological phases. (**I**) Western blotting examined the MMP8 protein level in critical/non-critical COVID-19 patients and healthy donors ($n = 3$). (**J**) qRT-PCR examined the MMP8 mRNA expression in critical/non-critical COVID-19 patients and healthy donors ($n = 10$). * represents $P < 0.05$, ** represents $P < 0.01$, ***represents $P < 0.001$, ****represents $P < 0.001$, ns represents no significance.

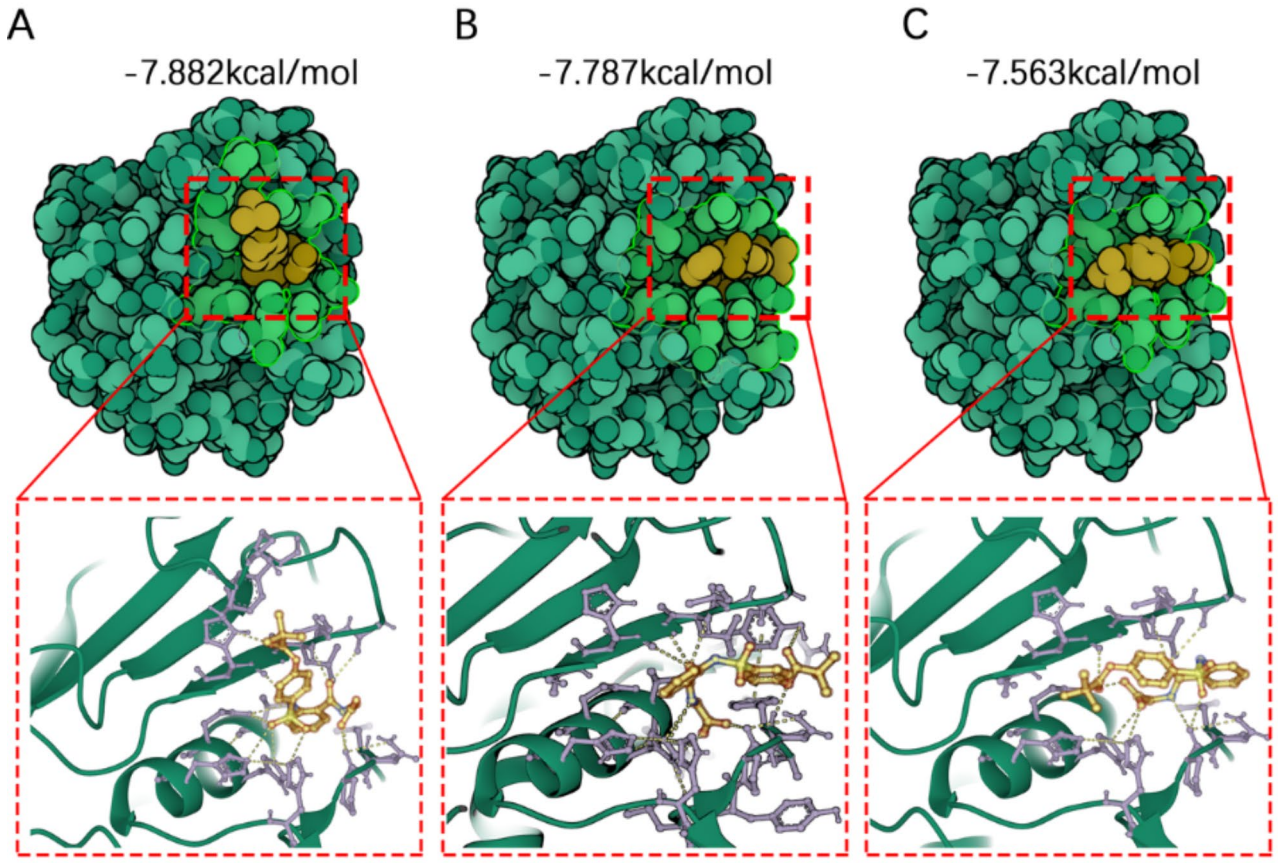

Fig. 2. Structure and SS binding site of MMP8. **A–C** The binding energy is – 7.828, – 7.811 and – 7.658 kcal/mol, respectively.

compared with those in the healthy group and non-severe COVID-19 group, and the distribution of myelocytes in severe COVID-19 group presented significant heterogeneity (Fig. 5D–F). Furthermore, the proportion of myelocytes with up-regulated MMP8 was elevated in 50–60 age group compared with that in 60–70 and 70–80 age groups, which indicated that younger trend of severe COVID-19 may be associated with the number of myelocytes with up-regulated MMP8 (Fig. 5G).

Receptor-ligand interaction network between MMP8-positive myelocytes and other cells

The cell-to-cell communication between different types of cell subpopulations is complex and proved to be crucial during virus infection progression and body inflammatory responses[39]. Therefore, an investigation was performed to have a further insight into MMP8-positive myelocytes and other cells in COVID-19 with the help of CellChat method based on healthy, non-severe and severe COVID-19 groups. The results of computational analysis uncovered that myelocytes presented more active cell-to-cell communication (Fig. 6A and B). As shown in Fig. 6C and D, the myelocytes could not only act as secreting cells to provide ligands, but also serve as target cells to accept the ligands released from other cells by receptors through multiple pathways. For example, myelocytes, $CD16^+$ monocytes, $CD16^-$ monocytes, NK cells, $CD4^+$ central memory T cells and γ-δ T cells were found to serve as the major secreting and receiving cells with the most outgoing and incoming signals in the cell-to-cell communication system. This suggested that there is a more frequent communicating network among cells in COVID-19. MMP8-positive myelocytes were the mainly supplier for Annexin, Resistin (RETN) and MHC-1, and the crucial target cells of MMP8-positive myelocytes were $CD16^+$ monocytes, $CD16^-$ monocytes, NK cells and neutrophils (Fig. 6C, E). From the receiver aspect, NK cells were the dominant cell type at incoming signaling, whereas RETN, GALECTIN, GRN and CD22 were listed in the top of ligands received by MMP8-positive myelocytes. Besides, immature B cells, $CD16^+$ monocytes and $CD16^-$ monocytes were the core secreting cells when MMP8-positive myelocytes served as target cells (Fig. 6D and E). In line with the above findings, RETN was regarded as a crucial signaling gene in the cell-to-cell communication of MMP8-positive myelocytes. Subsequently, the potential ligand-receptor pattern was evaluated using non-negative matrix factorization analysis to speculate the cell-to-cell communication manner of MMP8-positive myelocytes with other cells during COVID-19 progression (Fig. 6F). Three types of patterns were obtained according to the signal strength of ligand-receptor, and the contribution to different cell types and details of ligand-receptor

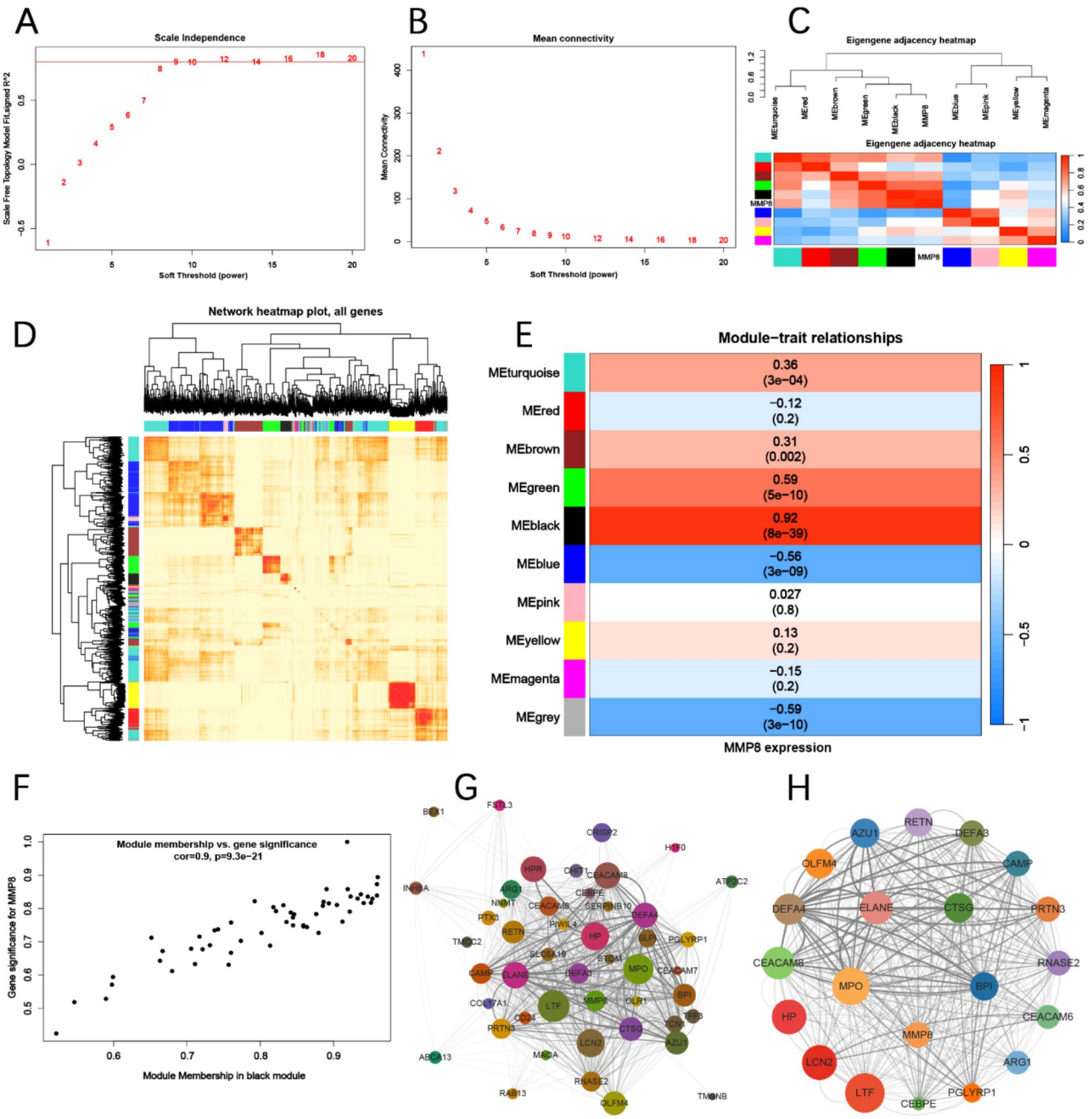

Fig. 3. Regulatory network of MMP8 in COVID-19 datasets. (**A**, **B**) WGCNA assessing the soft-threshold power. (**C**–**E**) Heatmaps presenting eigengene adjacency and correlation network of the 55 target DEGs, as well as module trait of MMP8. (**F**) Correlation analysis of module membership and MMP8 expression significance. (**G**, **H**) PPI network indicating the interactions between target genes.

pairs of these patterns were clustered (Fig. 6G). The $CD16^{-}$ monocytes, $CD16^{+}$ monocytes, neutrophils and myelocytes were observed to compose the communication pattern 2 occupying RETN signaling pathway. In that case, the following analysis was brought into to investigate the details of cell-to-cell communication pattern and the expressions of pattern member genes. According to Fig. 6H, MMP8-positive myelocytes served as the only sender cell of RETN-Toll-like receptor 4 (TLR4) communication pattern, and $CD16^{+}$ monocytes, $CD16^{-}$ monocytes and neutrophils acted as target cells. As for RETN-adenylyl cyclase-associated protein 1 (CAP1) pattern, almost all the cell types could simultaneously act as both the ligand provider and receptor. The results of pattern member gene expression analysis showed that MMP8-positive myelocytes were in the charge of RETN secretion presenting a high expression of RETN. TLR4 was mainly expressed in $CD16^{+}$ monocytes, $CD16^{-}$ monocytes and neutrophils, while the expression of CAP1 was discovered in all kinds of cells (Fig. 6I).

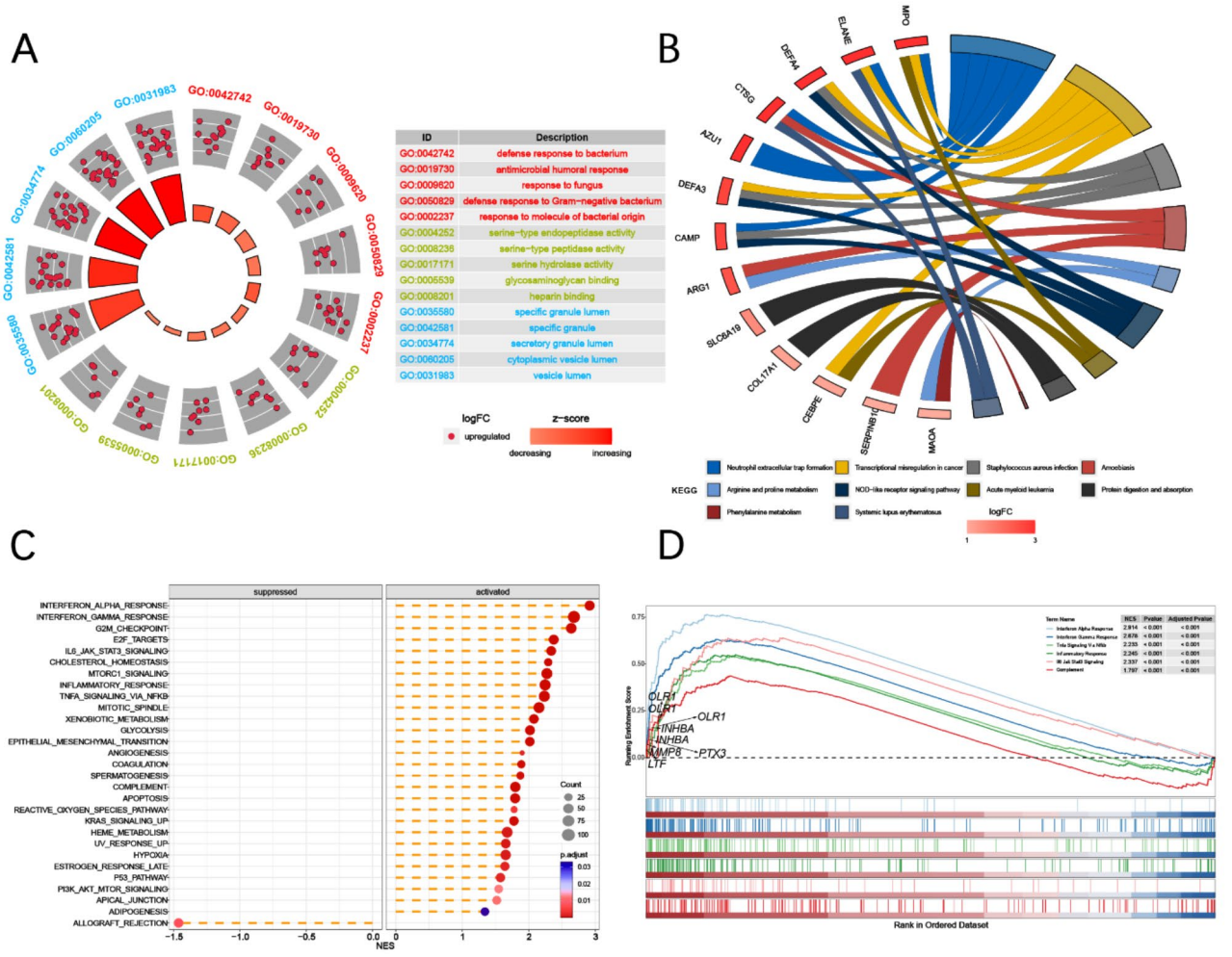

Fig. 4. Functional analysis of MMP8. (**A**, **B**) Enriched GO and KEGG terms for biological processes of MMP8. (**C**, **D**) GESA enrichment analysis illustrating MMP8 expression related functional processes.

In general, it was inferred that MMP8-positive myelocytes may interact with other cells through RETN-TLR4 and RETN-CAP1 ligand-receptor pathways to form a complex regulatory network, which participates in the progression of severe COVID-19.

Discussion

The outbreak of COVID-19 infection has resulted in great costs on public people health and social development[40]. The treatment strategy for COVID-19 is mainly focused on two aspects: seeking for benefit vaccines or targeted drugs to defend the intrusion of SARS-Cov-2 and settling the clinical symptoms of COVID-19 patients, such as fever, muscle pain, respiratory distress, pneumonia and fatigue[41]. Currently, BNT162b2 and ChAdOx1 nCov-19 vaccines are considered to have protection effects against COVID-19 infection according to their durations and infection-acquired immunity[42]. Novel findings demonstrated that Bananin, a derivative of adamantane, prevents the in vivo replication of virus via mediating helicase NSP13[43]. CR3022 monoclonal antibody is regarded as an available target on SARS-Cov-2 by blocking intercellular virus interaction[44]. Moreover, severe pneumonia is the most dangerous clinical presentation of COVID-19, which should be solved urgently. The combination of Tixagevimab and Cilgavimab presents effective therapeutic impacts on pneumonia syndrome of immunocompromised COVID-19 patients[45]. A phase II clinical trial conducted by Wang et al. indicated that better outcomes of pneumonia are found in COVID-19 patients at mild-to-moderate status[46]. Besides, SS is a potent anti-inflammatory drug commonly used in the clinical treatment of disorders in lung, artery, knee joint, etc. due to its inhibitory role in neutrophil elastase activity[4,8,47]. A recent study proved that SS is effective for COVID-19 by ameliorating pneumonia and respiratory distress syndromes[7].

According to the acquirement of the authors, recent literatures have mainly focused on the radiological and differential diagnosis, as well as the treatment in clinic, of COVID-19[48]. Few papers have reported the pathological progression mechanism as well as diagnosis and therapy molecular targets of COVID-19. In this

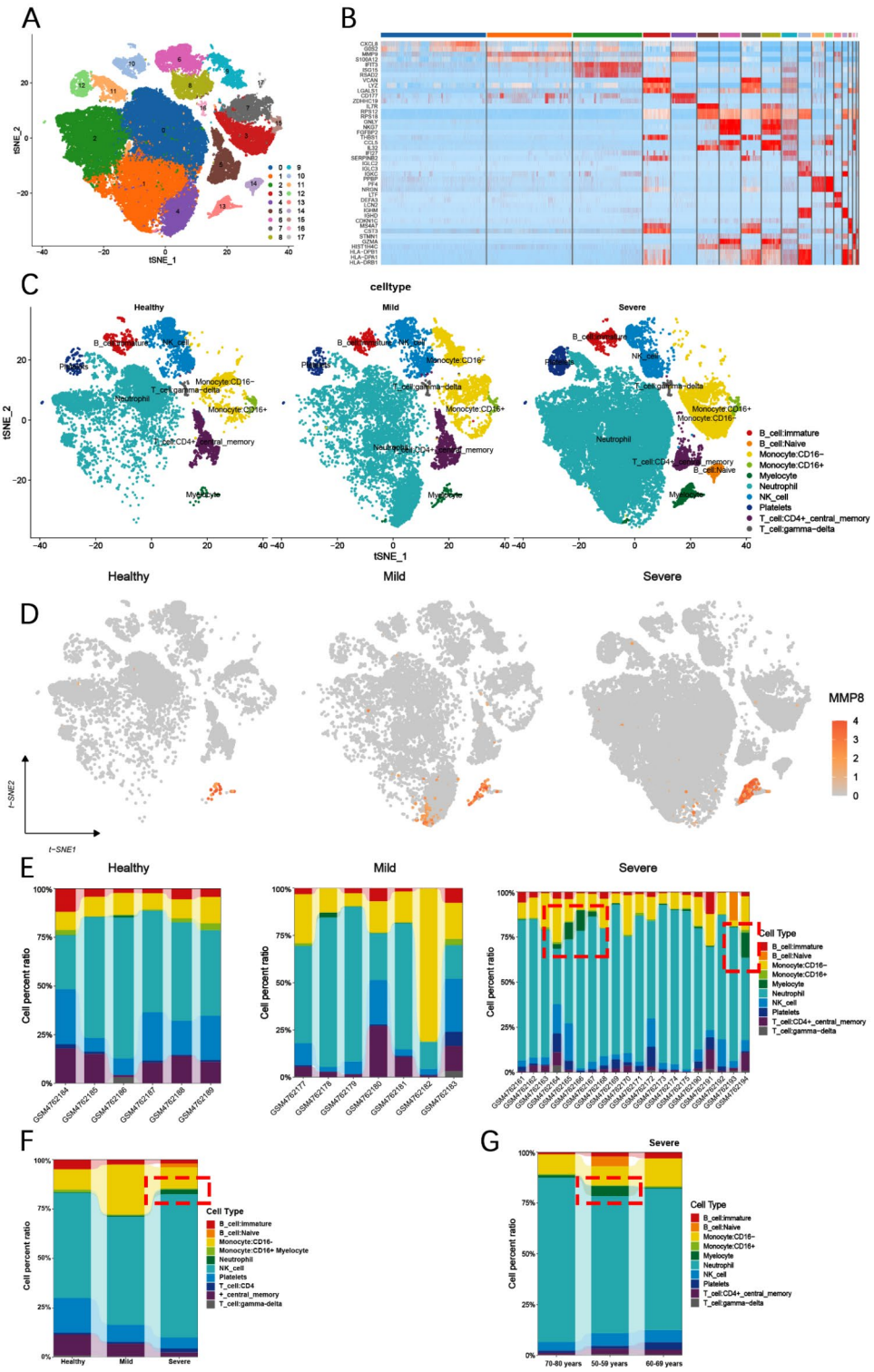

Fig. 5. ScRNA-seq presenting the landscape of MMP8-positive cells in COVID-19. (**A**, **C**, **D** and **F**) t-SNE plots showing cell distribution in the blood sample of COVID-19. (**B**) Heatmap presenting cell-situation related genes. (**E** and **G**) Relative proportions of different cell types for each dataset.

research, MMP8 was identified as the only DEG located in the cross point between severe and non-severe COVID-19 groups compared with healthy subjects, which was also a potential target for SS screening from PharmMapper drug target platform. The MMP8 expression was found to have a dramatic elevation with the aggravation of COVID-19 patients. Except for its core position in the regulatory network in which MMP8 cross-talked with other significant altered DEGs in COVID-19, the binding sites of MMP8 to SS were also

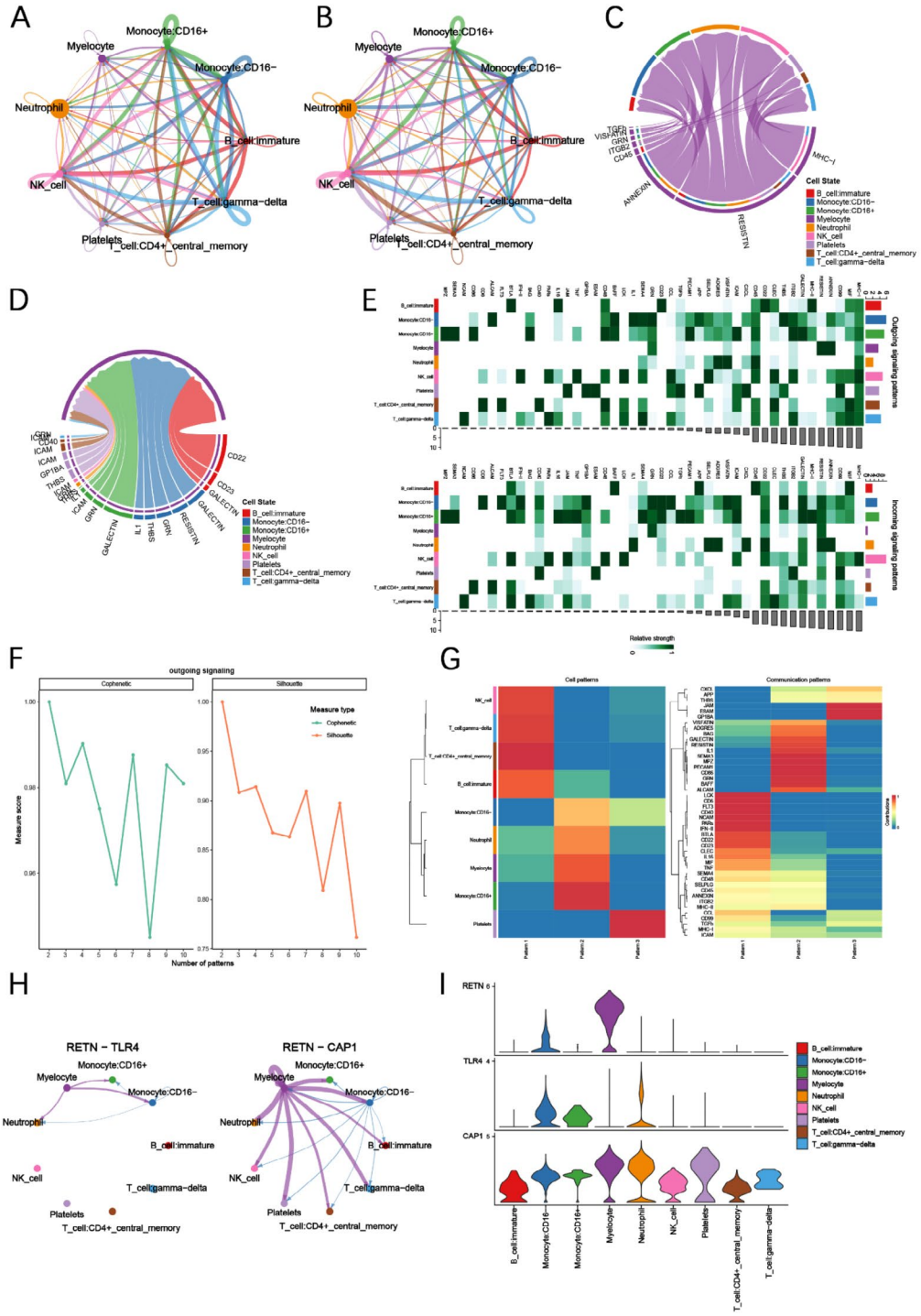

Fig. 6. Cell-to-cell communication analysis of MMP-8-positive myelocytes and other cells in COVID-19. (**A**, **B**) Circle chart presenting the number of interactions (**A**) or the total interaction intensity (**B**) between myelocytes and other types of cells. (**C**) Chord diagram indicating all significant interactions from MMP-8-positive myelocytes to others. (**D**) Chord diagram indicating all significant interactions from other cells to MMP-8-positive myelocytes. (**E**) Heatmap identifying the efferent or afferent contribution of all signals to various cells. (**F**) Non negative matrix factorization analysis of ligand-receptor data to infer the number of patterns based on two metrics implemented in the NMF R package, which include Cophenetic and Silhouette. An appropriate number of patterns for a pattern number range is the one where the Cophenetic and Silhouette values begin to drop abruptly. (**G**) Pattern clusters of ligand-receptor data obtained from the Cophenetic and Silhouette values between MMP-8-positive myelocytes and other types of cells. (**H**) Circle chart presenting significant interactions from MMP-8-positive myelocytes to others in RETN-TLR4 pathway and RETN-CAP1 pathway. (**I**) Violin plots showing the member gene expression in RETN pathway in various cell subtypes.

obtained. These findings indicated that the MMP8 alteration is correlated with and participates in COVID-19 pathogenesis, and MMP8 can act as a potential target of SS for COVID-19 therapy.

MMP8 is a member belonging to a diverse extracellular proteinase family which functions in a variety of biological cell development and homeostasis[49]. Evidence showed that the correlation between MMP8 and pneumonia is attributed to the fact that MMP8 works for defending the invasion of pathogens to keep the host healthy[50]. Michael et al. demonstrated the association of MMP8 with bacterial pneumonia by predictive models[51], corresponding to the findings of this study. Actually, scientists have discovered the increased level of MMP8 activation in the BALF sample of hospital-acquired pneumonia patients[52]. As a great support for this study, Pedro et al. illustrated that enhancing the effect of MMP2/MMP8-positive axis promoted the secretions of reactive oxygen species and lipid peroxidation leading to the dysfunction of lung tissue during COVID-19 progression[53]. The research of Hemant et al. concluded that the pharmacological inhibition of SS on spinal cord injury presented by depressing MMP8 expression, which reduced the infiltration of neutrophils in rat models[54], consistent with the validation results in this study, i.e., MMP8 served as a potential target of SS.

The results of functional enrichment analyses in this study suggested that MMP-8 was a key regulator of NET formation. Briefly, NET was a web-like extracellular structure that loads decondensed chromatin scaffold-assembled cytosolic or granule proteins[55]. The initial effects of NETs are indicated as trapping and protecting cells away from infectious sources, including virus, bacteria and fungi[56,57]. However, the overgoing of NET formation induced by uncontrolled neutrophil activation will serve as a contributor to the development of immune-related disorders[58]. Evidence pointed out that digesting the scaffold of NET DNA using DNase is an effective way to exacerbate inflammatory responses in acute lung injury experimental models[59]. Interestingly, Yu et al. validated significantly elevated expressions of myeloperoxidase-DNA and citrullinated histone H3, two marker genes for NET, in COVID-19 patients' blood samples, which stimulated NET formation in vitro[60]. A prospective cohort analysis on COVID-19 patients showed that there are excessive NET factors and increased neutrophil-platelet infiltration in pulmonary autopsies, and NET inhibitory factor ex vivo depresses the elevation of NET formation over baseline induced by COVID-19 plasma[61]. Furthermore, MMP8 oversecretion triggered by neutrophils is a harmful process that exacerbates human pulmonary tuberculosis and NET-stimulated infectious inflammation in the lungs[62,63].

With the supports of previous studies on the associations among MMP8, neutrophils, NET and COVID-19, the authors wondered that whether MMP8 regulates NET formation mainly through neutrophils during COVID-19. The results of scRNA-seq on COVID-19 peripheral blood samples indicated that the dramatical upregulation of MMP8 in myelocytes was correlated with the severe degree of COVID-19 and possessed obvious heterogeneity, although MMP8-potisive neutrophils presented a high cell rate. Myelocytes are a type of indicator leukocytes in the human blood, reflecting the immune function of the body[64]. As a kind of arsenal defending against diseases, myelocytes belong to a precursor cell of neutrophils and has a crucial role in immune regulation[65]. In this study, it was found that the proportion of myelocytes was increased sharply, and the distribution in severe COVID-19 group presented significant heterogeneity, especially in younger age group, compared with the healthy group and non-severe COVID-19 group. Therefore, it was inferred in this study that younger trend of severe COVID-19 may be associated with the number of myelocytes with up-regulated MMP8. However, an in-depth investigation should be conducted to verify such conclusions.

Cell-to-cell communication is considered as an important manner by which information can be transmitted from one cell to another with corresponding responses[66]. Under the regulatory cell-to-cell communication, the interaction between different cells generates protective impacts on body homeostasis and health to defend against extra intruders, such as virus, parasite or bacteria[67]. Ligand-receptor pattern is the common interacting way in the crosstalk between cells, and extracellular vesicle acts as the main medium transferring informatic substances[68]. Scientist demonstrated that the production of IL-10 derived from thymic epithelial cells triggers Ikaros and IRF8 activation in pre-T cells and promotes the differentiation into dendritic cells under physiological condition[69]. PD-1/PD-L1, a popular ligand-receptor pattern in tumor and immune cells, already guides the therapeutic direction of cancer diseases, blocking the intercellular immune communication by PD-1/PD-L1 inhibitors[70]. Emerging research emphasizes the crucial part of ligand-receptor-pattern-leaded cell-to-cell communication in the mechanism of immune derangement in COVID-19 progression. For instance, ANXA1 ligand on neutrophils promotes the migration of neutrophils to lung epithelial cells in the infected sites and acts on its FPR receptor for depressing the intrusion of SARS-Cov-2 virus[71,72]. Similarly, it was considered that the finding of this study was the first validation on the possible interaction between MMP8-positive myelocytes and other stromal cells by acting on RETN-TLR4 and RETN-CAP1 patterns. These evidences indicated ligand-receptor interaction patterns are potential drug checkpoints in COVID-19, RETN-TLR4 and RETN-CAP1 for example, and MMP8-positive myelocytes are core target cells in cell-to-cell communication.

In general, the alteration and great regulation value of MMP8 on COVID-19 pathogenesis are confirmed. MMP8 may serve as a potential biomarker for COVID-19 therapy as it binds to SS and has a critical impact on NET formation. Furthermore, MMP8-positive myelocytes are verified to act as important effector cells during COVID-19 progression and communicate with other functional cells depending on RETN-TLR4 and RETN-CAP1 ligand-receptor interaction patterns. Although these conclusions highlight the role of MMP8 in exploring COVID-19 therapeutic strategy, ambiguity and limitation still exist and need to be further explored. For example, the bulk sequencing captures a snapshot of the transcriptional alteration at a single time point, which may not reflect dynamic changes in gene expression or mutations over time, especially in response to treatments or environmental changes. Thus, more clinical characteristics and treatment strategies should be enrolled in subsequent studies to obtain dynamic changes of MMP8. Additionally, the scRNA-seq allows for the analysis of individual cells, the throughput could be lower compared to bulk sequencing methods, which may suffer from small sample sizes and could make it challenging to analyze large populations of cells efficiently. Thus, the single cell atlas studies should be carried out to detailly investigate the MMP8 expression difference. In

this study, MMP8 was identified as potential target of SS, however, it is not the only target. Kumar demonstrated that treatment with SS attenuated the IL-6 expression and iNOS, which is elevated in immune responses, inflammation, and apoptosis following spinal cord injury. However, SS also increases ANGPT-1 and decreases ANGPT-2 and NE expression after spinal cord injury to protect spinal from oxidative damage[73]. Therefore, molecular biology experiments are needed to perform to illuminate the specific relationship between SS and MMP8. Finally, the MMP8 expression distribution, functional role and pharmacological targets should be further validated using independent datasets or larger sample sizes.

Data availability

This manuscript did not generate new data, all relevant data were described in Methods and were obtained in GEO datasets.

Received: 23 July 2024; Accepted: 3 December 2024
Published online: 28 December 2024

References

1. Zhou, Y., Zhang, L., Xie, Y. H. & Wu, J. Advancements in detection of SARS-CoV-2 infection for confronting COVID-19 pandemics. *Lab. Invest.* **102**(1), 4–13 (2022).
2. Kaul, V. et al. Medical Education during the COVID-19 pandemic. *Chest* **159**(5), 1949–1960 (2021).
3. Sharma, A., Ahmad Farouk, I. & Lal, S. K. COVID-19: a review on the novel coronavirus disease evolution, transmission, detection, control and prevention. *Viruses* **13**(2). (2021).
4. Yu, X. et al. Sivelestat sodium hydrate improves post-traumatic knee osteoarthritis through nuclear factor-κB in a rat model. *Exp. Ther. Med.* **14**(2), 1531–1537 (2017).
5. Zhang, R. et al. Myocardial protective effect of sivelestat sodium in rat models with sepsis-induced myocarditis. *J. Thorac. Dis.* **14**(10), 4003–4011 (2022).
6. Kishimoto, M. et al. Sivelestat sodium and mortality in pneumonia patients requiring mechanical ventilation: propensity score analysis of a Japanese nationwide database. *J. Anesth.* **31**(3), 405–412 (2017).
7. Luo, M. et al. Sivelestat sodium for treatment of patients with COVID-19-associated acute respiratory distress syndrome in intensive care unit: a single-center retrospective cohort study. *Nan Fang Yi Ke da xue xue bao = J. South. Med. Univ.* **43**(8), 1259–1267 (2023).
8. Weng, J. et al. Sivelestat sodium alleviated lipopolysaccharide-induced acute lung injury by improving endoplasmic reticulum stress. *Gene* **884**, 147702 (2023).
9. Zandi, M. & Fani, M. Target genes used for biosensor development in COVID-19 diagnosis. *Biosens. Bioelectron.* **200**, 113924 (2022).
10. Lim, W. Y., Lan, B. L. & Ramakrishnan, N. Emerging biosensors to detect severe acute respiratory syndrome coronavirus 2 (SARS-CoV-2): a review. *Biosensors* **11**(11). (2021).
11. Lopes-Pacheco, M. et al. Pathogenesis of multiple organ injury in COVID-19 and potential therapeutic strategies. *Front. Physiol.* **12**, 593223 (2021).
12. Vianello, A. et al. The pathogenesis, epidemiology and biomarkers of susceptibility of pulmonary fibrosis in COVID-19 survivors. *Clin. Chem. Lab. Med.* **60**(3), 307–316 (2022).
13. Cione, E. et al. Neuron-specific enolase serum levels in COVID-19 are related to the severity of lung injury. *PLoS One.* **16**(5), e0251819 (2021).
14. Topp, G. et al. Biomarkers predictive of extubation and survival of COVID-19 patients. *Cureus* **13**(6), e15462 (2021).
15. Alay, H. & Laloglu, E. The role of angiopoietin-2 and surfactant protein-D levels in SARS-CoV-2-related lung injury: a prospective, observational, cohort study. *J. Med. Virol.* **93**(10), 6008–6015 (2021).
16. Wilk, A. J. et al. A single-cell atlas of the peripheral immune response in patients with severe COVID-19. *Nat. Med.* **26**(7), 1070–1076 (2020).
17. Primorac, D. et al. Adaptive immune responses and immunity to SARS-CoV-2. *Front. Immunol.* **13**, 848582 (2022).
18. Zhao, L. et al. Gasdermin D inhibits coronavirus infection by promoting the noncanonical secretion of beta interferon. *mBio* **13**(1), e0360021 (2021).
19. Luo, Y. et al. Identification of ZDHHC17 as a potential drug target for swine acute diarrhea syndrome coronavirus infection. *mBio* **12**(5), e0234221 (2021).
20. Mostafa, H. H. et al. Metagenomic next-generation sequencing of nasopharyngeal specimens collected from confirmed and suspect COVID-19 patients. *mBio* **11**(6). (2020).
21. Chen, X. et al. Next-generation sequencing reveals the progression of COVID-19. *Front. Cell. Infect. Microbiol.* **11**, 632490 (2021).
22. Wang, P. et al. Identification of potential vaccine targets for COVID-19 by combining single-cell and bulk TCR sequencing. *Clin. Transl Med.* **11**(5), e430 (2021).
23. Li, X. & Wang, C. Y. From bulk, single-cell to spatial RNA sequencing. *Int. J. Oral Sci.* **13**(1), 36 (2021).
24. Wang, T. et al. Integrating bulk and single-cell RNA sequencing reveals cellular heterogeneity and immune infiltration in hepatocellular carcinoma. *Mol. Oncol.* **16**(11), 2195–2213 (2022).
25. Lefol, Y. et al. TiSA: TimeSeriesAnalysis-a pipeline for the analysis of longitudinal transcriptomics data. *NAR Genom Bioinform.* **5**(1), lqad020 (2023).
26. Ritchie, M. E. et al. Limma powers differential expression analyses for RNA-sequencing and microarray studies. *Nucleic Acids Res.* **43**(7), e47 (2015).
27. Langfelder, P. & Horvath, S. WGCNA: an R package for weighted correlation network analysis. *BMC Bioinform.* **9**, 559 (2008).
28. Wu, T. et al. clusterProfiler 4.0: a universal enrichment tool for interpreting omics data. *Innov. (Camb).* **2**(3), 100141 (2021).
29. Bost, P. et al. Deciphering the state of immune silence in fatal COVID-19 patients. *Nat. Commun.* **12**(1), 1428 (2021).
30. Satija, R., Farrell, J. A., Gennert, D., Schier, A. F. & Regev, A. Spatial reconstruction of single-cell gene expression data. *Nat. Biotechnol.* **33**(5), 495–502 (2015).
31. Aran, D. et al. Reference-based analysis of lung single-cell sequencing reveals a transitional profibrotic macrophage. *Nat. Immunol.* **20**(2), 163–172 (2019).
32. Hu, C. et al. CellMarker 2.0: an updated database of manually curated cell markers in human/mouse and web tools based on scRNA-seq data. *Nucleic Acids Res.* **51**(D1), D870–D876 (2023).
33. Stubbington, M. J. T., Rozenblatt-Rosen, O., Regev, A. & Teichmann, S. A. Single-cell transcriptomics to explore the immune system in health and disease. *Science* **358**(6359), 58–63 (2017).
34. Jin, S. et al. Inference and analysis of cell-cell communication using CellChat. *Nat. Commun.* **12**(1), 1088 (2021).
35. Kijima, Y. et al. Suspected pneumonia caused by coronavirus disease 2019 after kidney transplantation: a case report. *Transplant. Proc.* 54(6):1547–1550. (2022).

36. Cheung, P. et al. Repression of CTSG, ELANE and PRTN3-mediated histone H3 proteolytic cleavage promotes monocyte-to-macrophage differentiation. *Nat. Immunol.* **22**(6), 711–722 (2021).
37. Chuang, H. C. et al. BPI overexpression suppresses Treg differentiation and induces exosome-mediated inflammation in systemic lupus erythematosus. *Theranostics* **11**(20), 9953–9966 (2021).
38. Liu, P. Y. et al. RNF128 regulates neutrophil infiltration and myeloperoxidase functions to prevent acute lung injury. *Cell. Death Dis.* **14**(6), 369 (2023).
39. Kostallari, E., Valainathan, S., Biquard, L., Shah, V. H. & Rautou, P. E. Role of extracellular vesicles in liver diseases and their therapeutic potential. *Adv. Drug Deliv. Rev.* **175**, 113816 (2021).
40. Fenollar, F. et al. Evaluation of the panbio COVID-19 rapid antigen detection test device for the screening of patients with COVID-19. *J. Clin. Microbiol.* **59**(2). (2021).
41. Perlman, S. Another decade, another coronavirus. *N. Engl. J. Med.* **382**(8), 760–762 (2020).
42. Hall, V. et al. Protection against SARS-CoV-2 after Covid-19 vaccination and previous infection. *N. Engl. J. Med.* **386**(13), 1207–1220 (2022).
43. Yadav, R. et al. Role of structural and non-structural proteins and therapeutic targets of SARS-CoV-2 for COVID-19. *Cells* **10**(4). (2021).
44. Tian, X. et al. Potent binding of 2019 novel coronavirus spike protein by a SARS coronavirus-specific human monoclonal antibody. *Emerg. Microbes Infect.* **9**(1), 382–385 (2020).
45. Nguyen, Y. et al. Pre-exposure prophylaxis with tixagevimab and cilgavimab (Evusheld) for COVID-19 among 1112 severely immunocompromised patients. *Clin. Microbiol. Infect.: Off. Publ. Eur. Soc. Clin. Microbiol. Infect. Dis.* **28**(12), 1654e1651–1654e1654 (2022).
46. Wang, Z., Chen, X., Lu, Y., Chen, F. & Zhang, W. Clinical characteristics and therapeutic procedure for four cases with 2019 novel coronavirus pneumonia receiving combined Chinese and western medicine treatment. *Biosci. Trends.* **14**(1), 64–68 (2020).
47. Zhou, Y., Li, X., Chen, H., Zhong, X. & Ren, H. Efficacy and safety of sivelestat sodium for the treatment of inflammatory response in acute Stanford type A aortic dissection: a retrospective cohort study. *J. Thorac. Dis.* **14**(10), 3975–3982 (2022).
48. Guarnera, A., Santini, E. & Podda, P. Idiopathic interstitial pneumonias and COVID-19 pneumonia: review of the main radiological features and differential diagnosis. *Tomography (Ann Arbor Mich).* **7**(3), 397–411 (2021).
49. Vandenbroucke, R. E. & Libert, C. Is there new hope for therapeutic matrix metalloproteinase inhibition? *Nat. Rev. Drug Discovery.* **13**(12), 904–927 (2014).
50. Gutman, H. et al. Matrix metalloproteinases expression is associated with SARS-CoV-2-induced lung pathology and extracellular-matrix remodeling in K18-hACE2 mice. *Viruses* **14**(8). (2022).
51. Gillette, M. A. et al. Biomarkers to distinguish bacterial from viral pediatric clinical pneumonia in a malaria-endemic setting. *Clin. Infect. Dis.: Off. Publ. Infect. Dis. Soc. Am.* **73**(11), e3939–e3948 (2021).
52. Hartog, C. M. et al. Pulmonary matrix metalloproteinase excess in hospital-acquired pneumonia. *Am. J. Respir Crit. Care Med.* **167**(4), 593–598 (2003).
53. da Silva-Neto, P. V. et al. Matrix metalloproteinases on severe COVID-19 lung disease pathogenesis: cooperative actions of MMP-8/MMP-2 axis on immune response through HLA-G shedding and oxidative stress. *Biomolecules* **12**(5). (2022).
54. Kumar, H. et al. Matrix metalloproteinase-8 inhibition prevents disruption of blood-spinal cord barrier and attenuates inflammation in rat model of spinal cord injury. *Mol. Neurobiol.* **55**(3), 2577–2590 (2018).
55. Lee, K. H. et al. Neutrophil extracellular traps (NETs) in autoimmune diseases: a comprehensive review. *Autoimmun. rev.* **16**(11), 1160–1173 (2017).
56. Lood, C. et al. Neutrophil extracellular traps enriched in oxidized mitochondrial DNA are interferogenic and contribute to lupus-like disease. *Nat. Med.* **22**(2), 146–153 (2016).
57. Branzk, N. et al. Neutrophils sense microbe size and selectively release neutrophil extracellular traps in response to large pathogens. *Nat. Immunol.* **15**(11), 1017–1025 (2014).
58. Papayannopoulos, V. Neutrophil extracellular traps in immunity and disease. *Nat. Rev. Immunol.* **18**(2), 134–147 (2018).
59. Scozzi, D., Liao, F., Krupnick, A. S., Kreisel, D. & Gelman, A. E. The role of neutrophil extracellular traps in acute lung injury. *Front. Immunol.* **13**, 953195 (2022).
60. Zuo, Y. et al. Neutrophil extracellular traps in COVID-19. *JCI Insight* **5**(11). (2020).
61. Middleton, E. A. et al. Neutrophil extracellular traps contribute to immunothrombosis in COVID-19 acute respiratory distress syndrome. *Blood* **136**(10), 1169–1179 (2020).
62. Nakamura, K., Nakayama, H., Sasaki, S., Takahashi, K. & Iwabuchi, K. Mycobacterium avium-intracellulare complex promote release of pro-inflammatory enzymes matrix metalloproteinases by inducing neutrophil extracellular trap formation. *Sci. Rep.* **12**(1), 5181 (2022).
63. Ong, C. W. et al. Neutrophil-derived MMP-8 drives AMPK-dependent matrix destruction in human pulmonary tuberculosis. *PLoS Pathog.* **11**(5), e1004917 (2015).
64. Bernstein, K. E. et al. Angiotensin-converting enzyme overexpression in myelocytes enhances the immune response. *Biol. Chem.* **395**(10), 1173–1178 (2014).
65. Bukowska-Strakova, K. et al. Heme oxygenase 1 affects granulopoiesis in mice through control of myelocyte proliferation. *Immunobiology* **222**(3), 506–517 (2017).
66. Diaz-Garrido, N., Cordero, C., Olivo-Martinez, Y., Badia, J. & Baldomà, L. Cell-to-cell communication by host-released extracellular vesicles in the gut: implications in health and disease. *Int. J. Mol. Sci.* **22**(4). (2021).
67. Mathieu, M., Martin-Jaular, L., Lavieu, G. & Théry, C. Specificities of secretion and uptake of exosomes and other extracellular vesicles for cell-to-cell communication. *Nat. Cell. Biol.* **21**(1), 9–17 (2019).
68. Yang, Q. et al. A proteomic atlas of ligand-receptor interactions at the ovine maternal-fetal interface reveals the role of histone lactylation in uterine remodeling. *J. Biol. Chem.* **298**(1), 101456 (2022).
69. Goruganthu, M. U. L., Shanker, A., Dikov, M. M. & Carbone, D. P. Specific targeting of notch ligand-receptor interactions to modulate immune responses: a review of clinical and preclinical findings. *Front Immunol* 11:1958. (2020).
70. Córdova-Bahena, L. & Velasco-Velázquez, M. A. Anti-PD-1 and Anti-PD-L1 antibodies as immunotherapy against cancer: a structural perspective. *Revista de investigacion clinica; organo del Hospital de Enfermedades de la Nutricion* 73(1):008–016. (2020).
71. Leslie, J. et al. FPR-1 is an important regulator of neutrophil recruitment and a tissue-specific driver of pulmonary fibrosis. *JCI Insight* **5**(4). (2020).
72. Qin, S. et al. Novel insight into the underlying dysregulation mechanisms of immune cell-to-cell communication by analyzing multitissue single-cell atlas of two COVID-19 patients. *Cell. Death Dis.* **14**(4), 286 (2023).
73. Kumar, H. et al. Neutrophil elastase inhibition effectively rescued angiopoietin-1 decrease and inhibits glial scar after spinal cord injury. *Acta Neuropathol. Commun.* **6**(1), 73 (2018).

Author contributions

Shunda Wang designed experiments, analyzed clinical samples and edited the manuscript. Zhenguo Liu performed testing, conducted data analysis and wrote the manuscript. All authors adopt the publication of the final manuscript.

Funding
This research received no specific grant from any funding agency in the public, commercial, or not-for-profit sectors.

Declarations

Competing interests
The authors declare no competing interests.

Ethical approval and consent to participate
Our study was conducted in accordance with the Declaration of Helsinki and approved by the Ethics Committee, Shaanxi Provincial People's Hospital (no. SPPH-LLBG-17-3_2).

Consent for publication
Not applicable.

Additional information
Supplementary Information The online version contains supplementary material available at https://doi.org/10.1038/s41598-024-82227-8.

Correspondence and requests for materials should be addressed to S.W.

Reprints and permissions information is available at www.nature.com/reprints.

Publisher's note Springer Nature remains neutral with regard to jurisdictional claims in published maps and institutional affiliations.